Article

Colloidal Stability of Graphene Oxide: Aggregation in Two Dimensions

MOAZZAMI GUDARZI, Mohsen

Abstract

Colloidal stability of graphene oxide (GO) is studied in aqueous and organic media accompanied by an improved aggregation model based on Derjaguin-Landau-Verwey-Overbeek (DLVO) theory for ultrathin colloidal flakes. It is found that both magnitude and scaling laws for the van der Waals forces are affected significantly by the two-dimensional (2D) nature of GO. Experimental critical coagulation concentrations (CCC) of GO in monovalent salt solutions concur with DLVO theory prediction. The surface charge density of GO is largely affected by pH. However, theoretical calculations and experimental observations show that the colloidal stability of the 2D colloids is less sensitive to the changes in the surface charge density compared to the classical picture of 3D colloids. The DLVO theory also quantitatively predicts the colloidal stability of reduced GO (rGO). The origin of lower stability of rGO compared to GO is rooted in the higher van der Waals forces among rGO sheets, and particularly, in the removal of negatively charged groups, and possibly formation of some cationic groups during reduction. GO also exfoliates in the [...]

Reference

MOAZZAMI GUDARZI, Mohsen. Colloidal Stability of Graphene Oxide: Aggregation in Two Dimensions. *Langmuir*, 2016, vol. 32, no. 20, p. 5058-5068

DOI : 10.1021/acs.langmuir.6b01012

LANGMUIR

Article

pubs.acs.org/Langmuir

Colloidal Stability of Graphene Oxide: Aggregation in Two Dimensions

Mohsen Moazzami Gudarzi*,†

Department of Polymer Engineering and Colour Technology, Amirkabir University of Technology, Tehran 15875-4413, Iran

Supporting Information

ABSTRACT: Colloidal stability of graphene oxide (GO) is studied in aqueous and organic media accompanied by an improved aggregation model based on Derjaguin-Landau-Verwey-Overbeek (DLVO) theory for ultrathin colloidal flakes. It is found that both magnitude and scaling laws for the van der Waals forces are affected significantly by the two-dimensional (2D) nature of GO. Experimental critical coagulation concentrations (CCC) of GO in monovalent salt solutions concur with DLVO theory prediction. The surface charge density of GO is largely affected by pH. However, theoretical calculations and experimental observations show that the colloidal stability of the 2D colloids is less sensitive to the changes in the surface charge density compared to the classical picture of 3D colloids. The DLVO theory also quantitatively predicts the colloidal stability of reduced GO (rGO). The origin of lower stability of rGO compared to GO is rooted in the higher van der Waals forces among rGO sheets, and particularly, in the removal of negatively charged groups, and possibly formation of some cationic groups during reduction. GO also exfoliates in the polar organic solvents and results in stable dispersions. However, addition of nonpolar solvents perturbs the colloidal stability at a critical volume fraction. Analyzing the aggregation of GO in mixtures of different nonpolar solvents and *N*-methyl-2-pyrrolidone proposed that the solvents with dielectric constants of less than 24 are not able to host stable colloids of GO. However, dispersions of GO in very polar solvents shows unexpected stability at high concentration (>1 M) of salts and acids. The origin of this stability is most probably solvation forces. A crucial parameter affecting the ability of polar solvents to impart high stability to GO is their molecular size: the bigger they are, the higher the chance for stabilization.

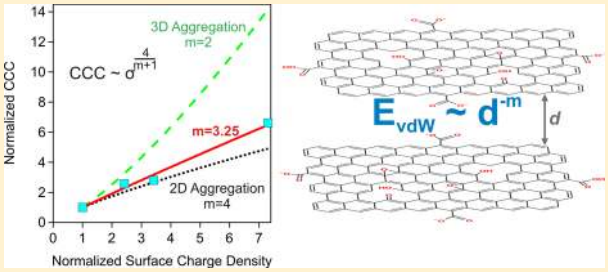

INTRODUCTION

Graphene oxide (GO) has been the center of attention during the past few years because it can be used as a precursor of graphene in a wide range of applications.[1−4] As an excellent candidate for solution processing of graphene-based materials, the colloidal stability of GO is crucial for controlling the performance and quality of final products. Increasing the ionic strength or decreasing the pH of aqueous dispersions of GO results in the coagulation of GO particles.[1,5−7] These observations have been reported since the first synthesis of graphite oxide by Sir Benjamin Collins Brodie,[8] where he stated in 1859 "*[graphite oxide] is insoluble in water containing acids or salts...*". It is now accepted that the origin of this stability is the electrostatic repulsion due to the overlapping of the electrical double layer around the GO sheets.[5−7,9] Colloidal properties of GO and graphene has been studied recently due to the practical importance of the stability of the graphenic dispersion.[6,7,10] However, what is missing in these studies is whether or not the 2D nature of GO (and graphene) affects the colloidal properties.[6,7] Looking at GO (and graphene) particles as 2D colloids may help us answer why dispersions of 2D particles (e.g., graphene) are more stable than their 3D counterparts (e.g., graphite).[10,11]

Due to the insulating nature of GO, chemical reduction of GO to an electrically conductive state has attracted great attention.[1,2,4,5] Since the seminal papers by Ruoff and his colleges[12] on the chemical reduction of GO, the stabilization of reduced GO (rGO) has been a crucial issue in the synthesis of chemically derived graphene.[13] Surfactant-free strategies are more attractive because they yield pure and more conductive products.[13] Most of the works on production of stable rGO dispersion are often based on the introduction of novel chemical pathways with little said on the origin of the stabilization.[13] The answer to the question of how chemical reduction of GO sheets makes them aggregate, may facilitate the developing of a general protocol for synthesis of stable rGO dispersions.[5]

In the realm of colloids and interface science, classical DLVO theory has been able to capture the colloidal properties of wide ranges of charged particles in polar media even for low dimensional colloids.[9,14,15] The essence of this theory is that the interaction energy among the colloids is the sum of the van der Waals (vdW) and electrostatic (EL) interactions.[9,15] Among the identical particles the vdW and EL interactions are always attractive and repulsive, respectively. Therefore, to make stable colloidal dispersions, the EL interactions must overcome the

Received: March 14, 2016
Revised: April 22, 2016
Published: May 4, 2016

DOI: 10.1021/acs.langmuir.6b01012
Langmuir 2016, 32, 5058−5068

vdW ones. However, the atomically thin nature of graphene families necessitates deriving appropriate force laws for 2D objects.

The aim of this paper is to provide a clear picture of factors controlling the stability of GO and rGO in polar media with a goal of developing a guideline to synthesize stable GO-based colloidal dispersions and possibly other 2D particles. In the first part of the paper, interactions between GO sheets are modeled. We look at the colloidal particles as ultrathin sheets covered with charged groups. As the required constants for calculation of the vdW forces among GO and rGO are not tabulated in the literature and data based on the surface energy measurements have been questioned recently,[16] we employed simplified Lifshitz theory to calculate the vdW forces.[14] By implementing the charging properties of GO in the DLVO theory, the aggregation of GO in polar solvents, especially water, is examined. In order to justify our recent observation of the unexpected high colloidal stability of GO in organic solvents,[17] we also include solvation forces in our model. In the second part, we experimentally examine the surface charge and colloidal properties of GO and rGO in aqueous media and compare them to the model. In the end, we provide a general guideline for preparation of stable GO-based colloids based on this research.

THEORETICAL BASIS

The stability of the colloidal particles is simply a matter of balance between attractive and repulsive forces.[9,15] Thus, what is required to predict the aggregation behavior of the colloidal particles, including GO and rGO, is to develop appropriate force laws for the so-called attractive and repulsive forces.

vdW forces are responsible for aggregation of colloids based on the DLVO theory.[14] The vdW interaction energy between two atoms scales with distance as follows:

$$\vartheta_{vdW} = -\frac{C}{d^6} \tag{1}$$

where d is the interatomic distance, and C is the vdW interaction (or dispersion) coefficient. C is a complex function of polarizability of the system, and it is usually computationally arduous to derive.[18] Under the assumption of perfect additivity for the vdW interactions, one can estimate the vdW potential energy among the macroscopic bodies of 1 and 2, where atoms are distributed according to a function, ρ, of position using the Hamaker approach as shown:[19]

$$W_{vdW} = \int_{v1}\int_{v2} \rho_1\rho_2\vartheta(d)\, dv_1\, dv_2 \tag{2}$$

In general, solving eq 2 results in a potential law that scales the separation distance of two interacting bodies as $1/d^m$, where $1 < m < 6$ depending on the geometry of the interacting bodies.[14,19] For two parallel atomically thin layers, eq 2 becomes[10]

$$W_{vdW} = -\frac{\pi A\rho_{2D}^2 C}{2d^4} \tag{3}$$

where ρ_{2D} is the surface density of atoms, and A is the area of the layers. The parameter ρ_{2D}^2C can be estimated from the surface energy of the materials.[10,14] However, the data on the surface energy and contact angle measurement of GO and graphene are scattered and often erroneous. For instance, in the simple case of the water contact angle on GO, the reported values vary between 30 and 68°.[20−22] The findings of Li et al.[16] questioned the previous measurements of wetting properties of graphenic films even more. Therefore, another approach based on Lifshitz theory for dispersion forces is pursued to estimate the vdW forces for GO and rGO.

The Hamaker constant between two semi-infinite media (1) and media (2) slabs interacting across a medium (3) can be estimated as follows:[14,23]

$$H_{Total} \approx \frac{3h\nu_e}{8\sqrt{2}} \times \frac{(n_1^2 - n_3^2)(n_2^2 - n_3^2)}{(n_1^2 + n_3^2)^{1/2}(n_2^2 + n_3^2)^{1/2}\{(n_1^2 + n_3^2)^{1/2} + (n_2^2 + n_3^2)^{1/2}\}} \tag{4}$$

where n is the refractive index in visible regime, h is the Planck constant, and ν_e is the main absorption frequency in the UV region. The zero-frequency term is neglected in eq 4, as this term cannot exceed 0.75 k_BT ($\approx$3.1 × 10^{-21} J, T is absolute temperature, and k_B is the Boltzmann constant), which is much smaller than the dispersion part. As a result, Hamaker constant can be estimated by having refractive indices of GO and rGO.

The average n of GO and rGO in visible regime are around 1.85 and 2.38, respectively.[24] Based on these data, and considering[14]

$$\nu_e = \nu_I\sqrt{3/(n^2 + 2)} \tag{5}$$

where ν_I is the absorption frequency of a Bohr atom (3.3 × 10^{15} s^{-1}) and n is the refractive index of interacting bodies, one can find H for GO and rGO across a vacuum as 136, 230 × 10^{-21} J, respectively. The H for graphite (n = 2.6−3.0) is thus between 260 and 310 × 10^{-21} J, which is close to the value tabulated in literature (238 × 10^{-21} J).[25] To examine the accuracy of above calculation, one can also find the dispersion coefficient (C) and compare it with more rigorous methods, assuming that[14]

$$H = \pi^2 C\rho_{3D}^2 \tag{6}$$

where ρ_{3D} is the volumetric atomic density. Considering the density of graphite is 2.27 g·cm^{-3}, the C of graphite is 22−25.3 au (210−242 × 10^{-80} J·m^6), which is within an impressive agreement with the value calculated based on a system of coupled quantum harmonic oscillators (28 au)[18] and the experimental one (24 au).[26] To the best of our knowledge, there is no data available for Hamaker constants of GO and rGO in the literature. Feriancikova and Xu reported a Hamaker constant of GO-water-quartz around 6.3 × 10^{-21} J based on surface energy measurements.[21] One should consider the fact that their estimation is for a GO−water−quartz system and should not be employed for a GO−water−GO system (the mistake that has been made in recent literature on GO aggregation studies).[7,27,28] The H for GO and rGO across the different liquids is also calculated and presented in Table 1.

It must be noted that eq 3 is derived for two atomically thin sheets, but the values obtained above are valid for two semi-infinite slabs. Using eq 3 for GO would result to an unrealistically high attraction energy, as the surface density of atoms in GO cannot be derived accurately. In fact, GO (and

Table 1. Hamaker Constant of GO and rGO Across Different Medias (×10^{21} J)

	vacuum	water	DMF	NMP	DMSO
GO	136	49	32	26	25
rGO	230	135	111	102	100

DOI: 10.1021/acs.langmuir.6b01012
Langmuir 2016, 32, 5058−5068

rGO) contains oxygenated functional groups out of plan of the graphenic backbone, making them not real 2D materials. Therefore, we model the vdW interactions between graphenic sheets using the potential law for two thin slabs as follows:[14,23]

$$W_{vdW} = -\frac{A \cdot H}{12\pi}\left(\frac{1}{d^2} + \frac{1}{(d + t_1 + t_2)^2} - \frac{1}{(d + t_1)^2} - \frac{1}{(d + t_2)^2}\right) \quad (7)$$

where t_1 and t_2 are the thicknesses of interacting slabs. The accuracy of this potential law was verified by comparing the vdW interaction of two graphene sheets (which is a perfect 2D material) using both eq 3 and eq 7 (Figure S1; Supporting Information (SI)). Both approaches result in approximately the same interaction energy, despite the fact that they are derived independently. As a result, the vdW interactions can be estimated using eq 7 for even atomically thin slabs.

The electrostatic double layer (EL) interactions between two identical interfaces is modeled using linearized Poisson–Boltzmann approximation for two planar surfaces as follows:[29]

$$W_{EL} = \frac{2\sigma^2}{\varepsilon\varepsilon_0\kappa}\exp(-\kappa d) \quad (8)$$

where σ is the surface charge density, ε_0 is the permittivity of vacuum, ε is the dielectric constant of solvent, and κ is the inverse of the Debye length, which is given by[29]

$$\kappa^{-1} = \sqrt{\frac{\varepsilon\varepsilon_0 k_B T}{2N_A e^2 I}} \quad (9)$$

where k_B is the Boltzmann constant, T is the absolute temperature, N_A is the Avogadro number, e is the elementary charge, and I is the ionic strength of solution. The ionic strength equals the salt concentration for solutions of monovalent salts. The electric surface potential (ψ) is calculated using the Grahame equation:[14]

$$\sigma = \frac{2\varepsilon\varepsilon_0\kappa k_B T}{e}\sinh\left(\frac{e\psi}{k_B T}\right) \quad (10)$$

In the above approximation, it is assumed that GO is opaque to the electric filed. In fact, it is considered as a thin slab with uniform surface charges, and the electrostatic interactions are independent of the thickness.[6] As the source of the negative charged groups in GO and rGO is from deprotonation of oxygenated groups, the pH of the environment significantly affects the colloidal stability.[6,27] This can be seen in the model above by assuming different surface charge density at different pH. We therefore used data of acid–base titration from Konkena and Vasudevan to derive σ versus pH.[30] The surface area of GO is assumed to be 1800 m^2/g in order to convert the charge density into surface charge density. The data fit numerically to derive σ at different pH (Figure 1). We found a good agreement between the titration data and our mobility measurements (Figure 1c,d). The same protocol is followed for rGO too.

Now the DLVO interactions between two graphenic sheets can be written as

$$W_{DLVO} = W_{vdW} + W_{EL} \quad (11)$$

When the energy barrier for the sheets to stick together becomes close to zero, fast aggregation happens.[29] The salt concentration reaches the critical coagulation concentration (CCC) when the following conditions are satisfied:

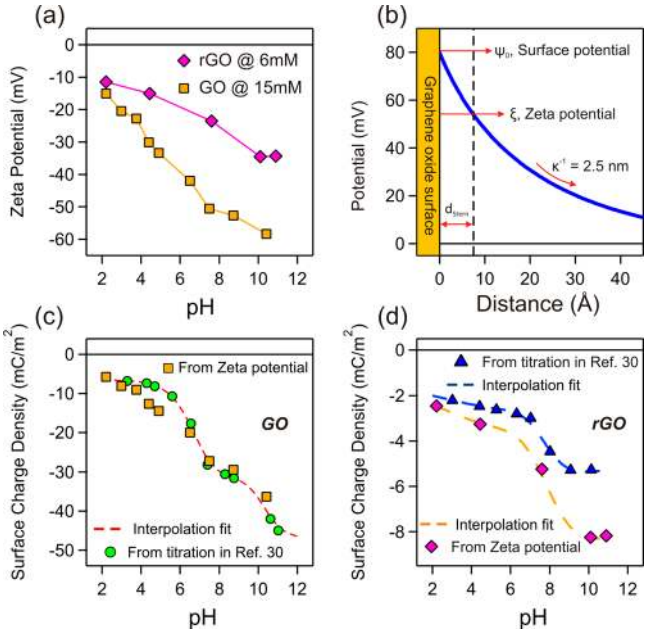

Figure 1. (a) Zeta potential of GO and rGO at fixed total ionic strength but different pH. (b) Potential profile of GO at ionic strength of 15 mM and pH = 10.4, obtained from eq 15. (c,d) Surface charge density of GO and rGO at different pH calculated from zeta potential measurement and titration data from Konkena et al.[30]

$$W_{DLVO} = 0; \quad \frac{\partial}{\partial d}W_{DLVO} = 0 \quad (12)$$

We applied these conditions to the equations above by inserting proper constants and physical parameters. One can then obtain the CCC for the different pH.

We have recently reported unprecedented stability of GO in polar aprotic solvents at high acid and salt concentrations.[17] It is suspected that this stability is originated from the solvation forces induced by structuring of solvent molecules confined between two approaching graphenic sheets. These forces are usually assumed to be oscillatory due to the ordering of the solvent molecules close to the surface.[14] However, one can model these forces by simple exponential as follows:[14]

$$W_s = -A_s \cdot \exp\left(-\frac{d}{\lambda}\right) \quad (13)$$

where A_s is the magnitude of the forces, and λ is the characteristic decay length of solvation forces and correlates with size of solvent molecules. The sizes of solvents are approximated by

$$\lambda = \left(\frac{M_w}{\rho \cdot N_A}\right)^{1/3} \quad (14)$$

where ρ and M_w are density and molecular weight of solvents, respectively. We estimate A_s from the work of Shih et al.[31] They simulated potential of mean force between pristine graphene and different solvents (NMP, DMSO, DMF, and water) which actually form an oscillatory energy potential. The height of the energy barrier (referred to β_1 in the work of Shih et al.[31]) is equated to A_s in our model, which about 0.13 $J \cdot m^{-2}$ for NMP, DMSO, and DMF and 0.2 $J \cdot m^{-2}$ for water, assuming surface area of graphene is 2600 m^2/gr.[31] However, it should be noted that, to the best of our knowledge, there is no theoretical

DOI: 10.1021/acs.langmuir.6b01012
Langmuir 2016, 32, 5058–5068

framework to estimate the magnitude of solvation forces based on the macroscopic properties.

MATERIALS AND METHODS

Preparation of GO Dispersion. Graphite flakes with an average size of 300 μm (Asbury Graphite Mills, US) were oxidized with the modified Hummers method based on previous work.[17] GO particles were dispersed in water or other organic solvents then sonicated for an hour using ultrasonic bath. Dispersions of GO in the polar protic solvents were prepared by solvent exchange method.[17] The final dispersions were centrifuged at 6000 rpm for an hour to remove large and/or nonexfoliated flakes. The concentration of GO in the stock dispersions was determined by drying certain volume of the dispersion and weighting the residue. The stock dispersions with concentration range of 1−2 mg/mL were used for further experiments. AFM (DualScope DS 95−200, DME, Denmark) analysis showed GO sheets are monolayered with average lateral dimension of 320 ± 24 nm (Figure S3).

Preparation of rGO Dispersion. GO dispersion in NMP (~1 mg/mL) were refluxed for 2 h in order to reduce GO solvothermally.[32] The rGO particles were filtered through a Teflon membrane (0.45 μm pore size) and washed with 1.0 N NaOH (aq) and then Milli-Q water. The rGO particles dispersed in water (pH ~ 10) and sonicated for an hour and then centrifuged at 6000 rpm for 10 min to remove exfoliated/aggregated particles. The resulting dispersion was used as stock solution for further studies. X-ray photoelectronic spectroscopy (Gammadata-scienta ESCA 200, USA) analyses showed C/O ratio in GO reduced from 2.4 to about 5 after solvothermal reduction.

Determination of Critical Coagulation Concentration. The protocol that has been used by Guo et al. was followed.[33] First the pH of the stock solutions was adjusted to the desired value using an aqueous solution of 0.1 M NaOH or 0.1 HCl. Then an appropriate amount of stock solution was added to electrolyte solutions with known ionic strength and pH in order to have 0.02 mg/mL of GO or rGO in final dispersion. The ionic strength of the solutions was adjusted using NaCl solution. At the end, the dispersions were left undisturbed overnight. Then they were centrifuged at 3000 rpm for 1 min, and the supernatant of dispersion was taken for the absorbance measurements. The absorbance at 230 nm (for GO) or 270 nm (for rGO) was normalized to the absorbance of GO or rGO at the same pH and no added salt. The ratios of the absorbances were considered as normalized concentrations, as the Beer−Lambert law is valid in the concentration range that measurements were performed. The normalized concentrations were plotted against the ionic strength, and the CCC of GO at respective pH is ascribed to the ionic strength at which the normalized concentration is half.[33] Determination of CCC should, however, be performed within a concentration range and time scale that slow aggregation is happening.

Determination of Critical Volume Fraction of Organic Solvents for Coagulation. The protocol described above was used except for sample preparation. Stock dispersions of GO in NMP were added to the mixture of NMP and nonpolar solvents (1-BtOH, THF, DCM, MeAc, Xylene) with known volume fraction. The final concentration of GO was set at 0.02 mg/mL. The normalized concentration of GO was obtained using the protocol above and plotted versus the volume fraction of organic solvents. The absorbances at 300 nm were considered for calculation of normalized concentration. The critical volume fractions were ascribed to the volume fraction at which the normalized concentration is half.

Zeta Potential Measurements. The zeta potential of the particles in aqueous dispersions was measured using a Zeta-Plus (Brookhaven Instruments Corporation, USA) at room temperature. The mobility of GO or rGO sheets at different pH and ionic strength was measured and converted to zeta potential using the Smoluchowski equation (Figure 1a). The surface charge densities were then calculated using the Grahame equation (eq 10). However, one needs to convert zeta potential to surface potential. To do so, we assumed the slipping plane located at 7 Å from the surface (Figure 1b). This is equal to Stern layer thickness (d_{Stern}) for sodium cations, recently measured by Brown et al.[34] To this end, the surface potentials were derived using the following equation:[29]

$$\psi_0 = \frac{4k_BT}{e}\,\mathrm{arctanh}\left[\exp(\kappa d_{Stern})\,\tanh\left(\frac{e\xi}{4k_BT}\right)\right] \quad (15)$$

where ψ_0 and ξ are the surface potential and zeta potential, respectively.

RESULTS AND DISCUSSION

General Feature of GO and rGO Aggregation. Figure 2a,c illustrates aqueous dispersions of GO and rGO at different

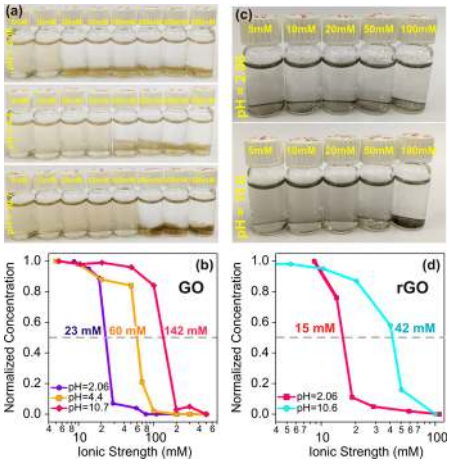

Figure 2. (a,c) Images of aqueous dispersions of GO (0.02 mg/mL) and rGO (0.01 mg/mL) at different pHs and ionic strengths, which were taken a day after preparation. (b,d) Normalized concentration of GO and rGO against ionic strength of dispersions at different pH. CCC is ascribed to the ionic strength at which the normalized concentration is half (dashed line).

ionic strengths at fixed pH of 2.06, 4.4 (not studied for rGO), and 10.7. GO particles start to aggregate at ionic strengths higher than 20, 50, and 100 mM for pH of 2.06, 4.4, and 10.7, respectively (Figure 2b). On the other hand, at a fixed ionic strength, there is a critical pH where fast aggregation of GO particles starts. For example, at the ionic strength of 50 mM, GO dispersions are stable at pH = 10.7 and 4.4 but start to aggregate at pH = 2.06. The same trend was also observed for the rGO dispersions. However, at the matching pH, rGO sheets aggregate at much lower ionic strength compared to GO. At basic solutions, GO sheets are even stable in the presence of 100 mM NaCl, whereas rGO is partially stable even at 50 mM NaCl. The origin of the lower stability of rGO will be discussed later.

DOI: 10.1021/acs.langmuir.6b01012
Langmuir 2016, 32, 5058−5068

The DLVO theory predicts these manners, i.e., instability in low pH or high ionic strength, for oxygenated colloidal particles such as GO and rGO. In the case of increasing the ionic strength, the electrical double layer shrinks due to the condensation of the counterions (Na^+). Consequently, at CCC, the vdW forces can overcome the repulsive DL forces, and the aggregation happens. Figure 3a shows the DLVO interactions between two GO sheets at pH = 4.5 but different NaCl concentrations, which supports the assumption above for the aggregation. On the other hand, when the ionic strength of the solutions is fixed, decreasing pH results in the protonation of the oxygenated groups of GO (or rGO), which significantly decreases the σ and strength of EL repulsion (Figure 3b). Therefore, at low enough pH (which depends on background ionic strength) again vdW overcomes the repulsive forces leading to the aggregation of the particles.

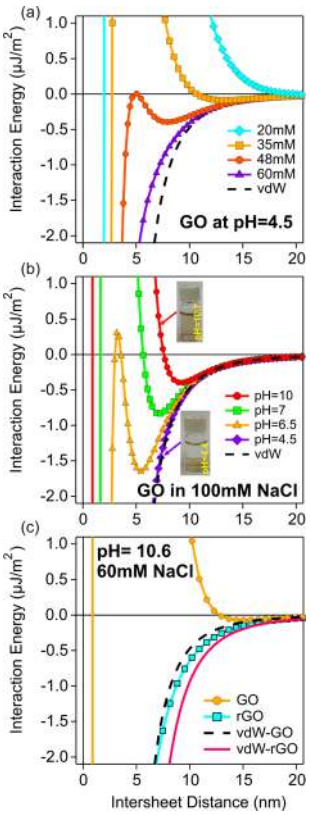

Figure 3. DLVO interaction energy between (a) two GO sheets at fixed pH but different ionic strength and (b) at fixed ionic strength of 100 mM but different pH. (c) DLVO interaction energy between two GO sheets and two rGO sheets at ionic strength of 60 mM and pH = 10.6. Surface charge density at different pH obtained from Figure 1c,d. The insets in panel b are GO dispersions (0.02 mg/mL) at 100 mM NaCl at pH = 10.7 and 4.4.

The aggregation of the particles was tracked by measuring the concentration of GO (or rGO) after adding salt, normalized against the initial concentration (see Methods for more details). A rapid decrease in the concentration is a sign of the start of fast aggregation regime. In line with our expectations, both GO and rGO are less prone to aggregate in the basic media as CCC increases with increasing pH (Figure 2b,d). At pH 4.4, CCC of GO is around 60 mM, which matches with the findings of Chowdhury et al.[7] and Zhao et al.[35] Increasing pH to 10.7 results in more than 2 times increase in CCC of GO. However, at pH = 10.7, CCC of rGO is more than 3 times lower than GO ones. This clearly shows significant impact of reduction of GO on the colloidal properties (see the next part for more details).

An interesting observation is the stability of both GO and rGO at pH = 2.06 (CCC_{GO} = 23 mM, CCC_{rGO} = 14 mM). If the surface charges are just originated from the oxygenated groups (pK_a = 3−9),[30] at such a low pH, the particles must be uncharged. For the case of rGO, it is even more puzzling as the pK_a of oxygenated groups in rGO is around 8, and it is very unlikely that some extra charged groups form during reduction.[30] A possible explanation could be the presence of sulfate groups in GO.[36] The sulfur content in GO can vary in the range of 2 to 0.4% even after extensive purification, which roughly equals 15−5 mC/m^2, which agrees with the surface charge density of GO obtained in this work at pH = 2.06 (5.2 mC/m^2).[36] Covalently bonded sulfate groups are hard to remove during reduction.[36] Therefore, they are perhaps responsible for the stability of rGO at low pHs.

On the Stability of rGO Dispersions. GO turns black during reduction, which is a clear sign of changing its optical properties, including an enhanced refractive index[24] (Figure 2a,c). The Hamaker constant of GO sheets in water increases about 3 times after reduction (Table 1). Reduction of GO also decreases the surface charge density even up to 10 times compared to GO. As $W_{EL} \approx \sigma^2$, this means more than 100 times decrease in the magnitude of the electrostatic forces (eq 8, Figure 1c,d). This already elucidates the origin of instability of GO during the reduction: the attractive forces between the graphenic sheets strengthen, whereas the repulsive ones decrease significantly (Figure 3c). Enhanced vdW interactions in rGO are possibly stemmed from the restoring of the conjugated structure of graphene.

The explanation above is against the picture that is usually proposed for the instability of rGO, where it is wrongly attributed to the phenomena of "rGO becoming more hydrophobic" or "less water-soluble" and "$\pi-\pi$ stacking" of rGO sheets.[12,13] These terms are usually ambiguous and confusing. For instance, using the term $\pi-\pi$ stacking does not describe the underlying forces involved in aggregation.[37] It is accepted that the vdW forces have considerable contribution in the stacking of the large aromatic molecules, and in the case of the stacking of graphene to graphite is almost the sole driving force.[18,38] Apart from the physical origin of the instability of rGO, it is more interesting to provide a guideline for the preparation of stable rGO colloids based on these findings.

Experimentally, it is challenging to design and control aggregation of rGO as the reducing agents and reaction byproducts usually act as ionic species in media, which not only change the total ionic strength of environment but also can interact and neutralize rGO.[12,13] For example, in a seminal paper by Stankovich et al.[12] on the synthesis of rGO, the reducing agent (hydrazine, $N_2H_4{\cdot}H_2O$) concentration was more than 300 mM, which not only changes the background ionic strength of solution, but also the chemical binding of hydrazine to GO decreases the surface charge density of the final product. A noticeable amount of nitrogen is found in hydrazine -reduced GO, which act as cationic sites especially at low pH.[12,39] Finding slightly positive zeta potential at very low pH is another sign of the presence of cationic groups in hydrazine-reduced GO, which hampers the colloidal stability of it.[5,30]

The above analysis is telling us that the main factor leading to the aggregation of rGO is the significant decrease in the

DOI: 10.1021/acs.langmuir.6b01012
Langmuir 2016, 32, 5058−5068

number of charged groups upon reduction and probably the formation of some cationic groups too. Therefore, any chemical method that preserves negatively charged groups (e.g., carboxyl and sulfate) but meanwhile removes the oxygen groups is potentially able to use the surfactant-free method to synthesize stable rGO dispersions. Basic reducing agents, such as hydrazine, have high potential to interact with carboxyl groups (the main source of charges in rGO) and neutralize them.[5,13] Therefore, acidic or neutral reducing agents have higher potential for making surfactant-free dispersions. In general, one should avoid adding extra ionic species to the reducing media. Moreover, higher pH (one or two units higher than pK_a of rGO, which is about 8) is always welcomed to ensure full ionization of oxygenated groups. This indeed matches very well with successful chemical recipe for making stable rGO dispersions in the literature where acidic reducing agents such as ascorbic acid,[40] polyphenols (including many natural antioxidants such as Luteolin, Apigenin),[41] Formamidinesulfinic acid,[42] amino acids,[43] sugars such as glucose, fructose, and sucrose[44] were used.

DLVO Prediction for Aggregation. One can calculate the CCC of GO (or rGO) dispersions by solving eqs 7−12. To do so, two main parameters are required to insert in those set of equations, which are surface charge density (σ) and thickness of the nanosheets (t). We will discuss the effect of t later; but let us consider the d-spacing of GO as the effective thickness (around 6.7 Å obtained from the X-ray diffraction pattern).[17] The other parameter, i.e., σ, is pH dependent. At fixed pH of 4.4, σ for GO is 12.6 mC/m^2, derived from the electrophoresis mobility measurements. (Figure 1c) Based on these values, the calculated CCC is 79 mM. This agrees with experimental CCC of GO at the pH of 4.4, i.e., 60.5 mM. Quantitative accurate prediction of aggregation behavior of GO using DLVO theory is rare in previous works.[6,7,10,27,28,35] For instance, Chowdhury et al.[7] overestimated CCC about 3-fold.

Calculation of CCC can be extended for different pH if the dependency of σ on pH is known. As mentioned in the Theoretical Basis section, we employed the titration data and interpolated them to have σ as a function of pH[30] (Figure 1c,d). CCC versus pH can be calculated by solving eqs 7−12 numerically. However, during these analyses, a set of interesting scaling laws were derived. In the case of GO, one obtains:

$$\mathrm{CCC}_{\mathrm{GO}} \sim \sigma^{0.874} \tag{16}$$

A similar power law was obtained for rGO but with different exponent (0.838). The origin and the impact of such scaling behavior will be discussed later. One can directly calculate CCC versus pH by applying the fitting data of σ as a function of pH into the above scaling law.

Now, let us consider another parameter, i.e., thickness of nanosheets. Increasing the thickness of the sheets enhances vdW forces, and, as a result, stronger electrostatic forces are required for stabilization. We calculated the CCC of GO at a fixed σ for different thicknesses within the range of 4 to 30 Å (the possible range for GO sheets). The following scaling law is obtained:

$$\mathrm{CCC}_{\mathrm{GO}} \sim t^{-0.66} \tag{17}$$

CCC of GO is thus affected by the level of exfoliation; for instance, the CCC of trilayered GO is predicted to be almost half that of monolayered GO. The scaling power for rGO and graphene decreases to about −0.75 ($\mathrm{CCC}_{\mathrm{rGO}} \sim t^{-0.75}$), meaning that their colloidal stability is more sensitive to exfoliation level. The reported thickness for monolayered GO varies from a lower limit of 6 Å to even more than 12 Å.[1,4,5,12] Moreover, the thickness of GO also depends on oxidization level.[45]

Based on the scaling laws above, we calculated CCC of GO for different pH and for different thickness of GO (lower limit of 5 Å and upper limit of 10 Å) (see S.I.). The result is illustrated in Figure 4. Moreover, the experimental data from this work and other references are included.[7,27,35,46,47] One can realize that the DLVO theory captures well the trend of GO aggregation even quantitatively. An interesting feature of this analysis is that GO aggregation is very sensitive to pH, especially when passing from slightly acidic to slightly basic. For instance, $\mathrm{CCC}_{\mathrm{pH=5}}$ is almost 3 times lower than $\mathrm{CCC}_{\mathrm{pH=8}}$. This finding can have an significant impact on GO storage as GO self-generates proton during interaction with water.[48] Therefore, slightly basic dispersion of GO can become slightly acidic over time and becomes much more sensitive to ionic impurities.

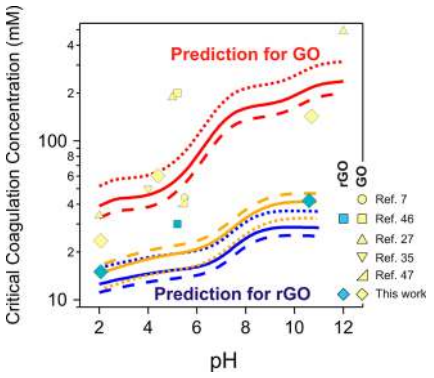

Figure 4. Dependence of CCC on pH: the experimental CCC of GO and rGO, measured in this work and other works (for monovalent salts) at different pHs, are illustrated by different symbols. Solid and dotted lines are calculated CCC based on DLVO theory, using scaling laws derived in this work and titration data (Figure 1c). Calculation were done for three different thickness of GO: 6.5 Å (solid line), 5 Å (upper limit), and 10 Å (lower limit). Calculations for rGO were done using both titration data (blue lines) and surface potential measurements (orange lines) (Figure 1d). Different thickness for rGO were also considered: 4 Å (solid lines), 3.4 Å (upper limit), and 5.5 Å (lower limit).

One can also find the pH-dependency of CCC of rGO in the same fashion. The data from the work of Konkena et al.[30] (they used hydrazine reduced GO) and mobility measurements were used. The σ of solvothermally reduced GO in the whole pH range is more negatively charged than that of hydrazine-reduced GO (Figure 1d). Figure 4 shows the CCC of rGO at different pH. The CCC drops significantly as pH decreases from 9 to 6, which is not surprising because most of the charges on rGO originated from the remaining carboxyl groups after the reduction with pK_a around 8.[30] Based on this calculation, the CCC of the rGO is about 6 times lower than the GO at pH = 7. This implies that the colloidal stability of rGO is much more sensitive to ionic species compared to GO.

The DLVO theory has extensively been employed to predict the colloidal properties of carbon nanomaterials such as CNTs,[31,49] fullerenes[50] and graphenes.[7,27,28,46,47,49] For instance Shih et al.[49] calculated the interactions between surfactant coated SWNTs and graphene with an improved DLVO theory for nanotubes and ultrathin sheets. Although in

DOI: 10.1021/acs.langmuir.6b01012
Langmuir 2016, 32, 5058−5068

many of these studies, behavior of carbonic colloids can be captured even quantitatively, the issue of impact of dimensionality of colloids on aggregation behavior is rarely discussed. In the case of aggregation of GO and rGO, most of studies are limited to measurement of aggregation or deposition of GO or rGO in aquatic environments, and when it comes to modeling the colloidal properties, these particles are assumed to be spherical.[7,21,27,28,46] Apart from this erroneous assumption and assigning very low Hamaker constants to GO, the effect of pH on the aggregation behavior of GO and rGO has not been argued extensively.[7,27] In the next part, the missing part of the effect of the dimensionality of colloids on the aggregation behavior is presented.

Aggregation of 2D Objects. What makes GO (and other 2D colloids) distinct from the classical spherical colloids within DLVO theory framework, is the shape and scaling of vdW forces (and EL forces in a sense that Derjaguin approximation is not required).[14] How the dimensionality of colloids affects their aggregation behavior? As mentioned in the theoretical part, solving eq 2 results in energy potential scaling laws of d^{-m} where power-law exponent (m) depends on dimensionality. For instance for two individual atoms m is 6, for two parallel 2D sheets reduces to 4 and for two surfaces finally reaches to 2.[14] Now, let us consider:

$$W_{vdW} = -\frac{\text{constant}}{d^m} \tag{19}$$

Considering eqs 8 and 11, and then solving eq 12, we obtain

$$CCC \sim \sigma^{4/m+1} \tag{20}$$

Also, the separation distance at the energy barrier (d_{max}) is

$$d_{max} = m \cdot \kappa^{-1} \tag{21}$$

For the perfect 2D object, i.e., $m = 4$, CCC scales σ by a power of 0.8, whereas for the 3D objects CCC scales σ by a power of 1.33.[51] However, we calculated a scaling power of 0.874 for GO. The same analysis for the case of rGO and graphene gives a scaling power of 0.838. Therefore, m for GO and graphene is 3.58 and 3.77. The origin of deviation from perfect 2D is hidden in the shape of the function that is used for vdW modeling (Figure S2). Surprisingly, this finding matches well with the recent calculation of Ambrosetti et al.,[52] where they found m between 3.5 and 3.75 for graphene (see SI).

Is it then possible to track the flatness of GO particles in their aggregation behavior? To answer that, we calculate σ and CCC of GO and rGO at different pH and plot normalized CCC versus σ (normalized to values at pH = 2.06 for both GO and rGO) (Figure 5). The data lie between two extreme cases of 2D and 3D ones, but closer to the 2D state. Fitting the data gives a scaling power of $m = 3.25$. Therefore, the 2D nature of GO can be tracked in the aggregation behavior of colloids. This implies the 2D colloids are less sensitive to the changes in charges on the surface. These findings put question on the true dimensionality of GO and probably other 2D colloids in solution. Considering finite thickness for GO (or rGO) in the calculation of the vdW interactions results in dimensionality lower that perfect 2D. However, experimental dimensionality ($m = 3.25$) is even lower than the theoretical expectation. Other factors such as rapid orientation, flexibility, crumpling, and wrinkling of the GO sheets might be the origin of deviation from perfect 2D behavior.[53−55] More experimental and theoretical works on obtaining dimensionality of 2D objects

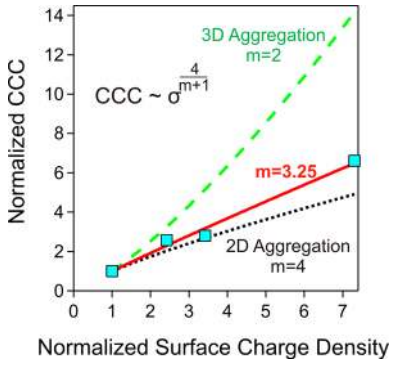

Figure 5. Normalized CCC against normalized σ: normalization was done against CCC and σ at pH = 2.06. Surface charge density for each pH was derived directly from surface potential measurements (Figure 1c,d).

is expected to shed light on the old issue of true dimensionality of ultrathin membranes.[53,54]

Another interesting observation in the modeling of the aggregation of the 2D colloids, is that d_{max} is m times larger than κ^{-1}[51] (eq 21, Figure 6). While scanning the literature of

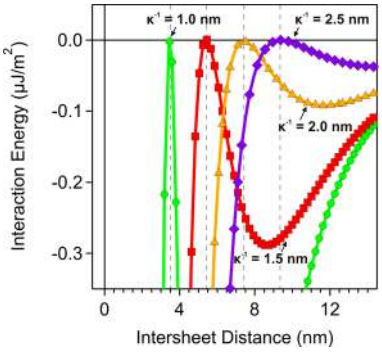

Figure 6. Interaction energy between two GO sheets at CCC for the different Debye lengths (i.e., ionic strength): κ^{-1} fixed to a desire value and σ at which the potential barrier is zero were used to produce energy potential. The dashed lines are the positions of potential barriers.

the colloidal properties of the 2D colloids, we realized that in the early 1960s, an unusual swelling of clays was observed by Norrish[56] and later by Walker.[57] Both of them observed the interlayer spacing of clay at low ionic strength linearly increases by increasing the Debye length (κ^{-1}). Another fact that catches less attention is that in both cases, the interlayer spacing is exactly equal to $3.66\kappa^{-1} + d_0$. Norrish[58] later tried to justify quantitatively the proportionality coefficient of 3.66 based on the DLVO theory but failed simply because of a wrong assumption he made during his calculation. We believe this proportionality coefficient is directly connected to the 2D nature of clays. However, this must be checked for swelling properties of GO and other 2D crystals.[11,45,59] Unusual gelation and swelling of rGO might originate from the unique DLVO interactions among the rGO sheets, too.[60] Therefore, further elaboration on modeling of the swelling and stacking of the 2D colloids based on the DLVO theory or modified versions may provide a clear picture. It should be noted that in concentrated dispersions, other interactions such as excluded volume interaction may affect the behavior of GO-based dispersions,

DOI: 10.1021/acs.langmuir.6b01012
Langmuir 2016, 32, 5058−5068

but DLVO interaction among GO sheets still provides a basis for more complicated models.

Solvent-Induced Stabilization. The DLVO theory is a mean-field theory and what is especial in calculation of the first part is just physical constants used for dispersing media, i.e., water. Interactions among GO sheets in any other liquid can be calculated in the same but relevant dielectric constants, and refractive indices should be employed in the model. In this section, we will try to explain a basis for why GO is not stable in nonpolar solvents using DLVO theory. An attempt is also made to clarify the unforeseen high colloidal stability of GO in some polar solvents at very high electrolyte concentration.[17]

The driving force for aggregation of GO sheets is vdW forces. The magnitude of vdW forces is similar for most of the organic solvents as the refractive indices of the organic solvents vary in the shallow range (1.3−1.6). Therefore, the Hamaker constants of GO interacting in organic solvents are within the same magnitude (Table 1). As a result, the attractive forces are also in the same magnitude, if not lower, of that for a GO−water−GO system. Thus, the aggregation of GO sheets in nonpolar solvent should originate from weakened repulsive EL forces.

In nonpolar solvents, the charging behavior of GO sheets significantly changes. It is agreed that the ionization constant (pK_a) of the acidic groups (which are the main source of charges on GO) shift to much higher values in organic solvents compared to water.[61] Generally, the lower ε is, the higher pK_a is. In addition, in nonpolar solvent, the Bjerrum length (the distance where the electrostatic interaction between two charges is equal to thermal energy) is much larger than the one in water and, as a result, dissociation of acidic groups is much less probable.[61] These significantly reduce σ and the EL forces. When these two effects (low σ and very high κ^{-1} due to low solubility of salts in nonpolar solvents) combine, the energy barrier declines and aggregation is inevitable.

Indeed our observations and others showed there is limit for polarity of "good solvents" for GO.[17,62] For instance, we found that GO does not form a stable colloid in THF (ε_{THF} = 7.5) or dicholorobenzene (ε_{DCB} = 10), whereas acetone ($\varepsilon_{acetone}$ = 20.7) is a good medium.[17] Another proof that there is critical polarity for the liquids that can present electrostatic stabilization for GO is aggregation of GO in polar solvents upon addition of (miscible) nonpolar solvents. Figure 7a shows the dispersions of GO in a mixture of NMP and different nonpolar solvents (1-BtOH, THF, DCM, MeAc). At low content of nonpolar counterpart, the dispersions are stable. However, upon increasing the fraction of nonpolar solvents, GO sheets start to aggregate. We tracked the normalized concentration of GO at the different volume fractions of the nonpolar solvents (Figure 7b) and derived the critical aggregation volume fraction (φ_{crt}). φ_{crt} for different solvent sequences as follows:

$$\text{1-BtOH} > \text{THF} \sim \text{MeAc} > \text{DCM} > \text{Xylene}$$

It is interesting that this trend follows the order of ε of the solvents. ($\varepsilon_{1\text{-BtOH}}$ = 17.8, ε_{THF} = 7.6, ε_{DCM} = 8.93, ε_{MeAc} = 7.3, ε_{Xylene} = 2.6) Therefore, it supports the idea of the presence of a critical ε for stabilization of GO. Calculations based on Fuoss' theory indeed show that just liquids with ε > 13 can provide sufficient electrostatic forces for stabilization.[61,63] Now we try to derive the critical ε for stabilization. One can estimate ε of the solvent mixtures as follows:[64]

$$\ln(\varepsilon_m) = \varphi_1 \cdot \ln(\varepsilon_1) + \varphi_2 \cdot \ln(\varepsilon_2) \quad (22)$$

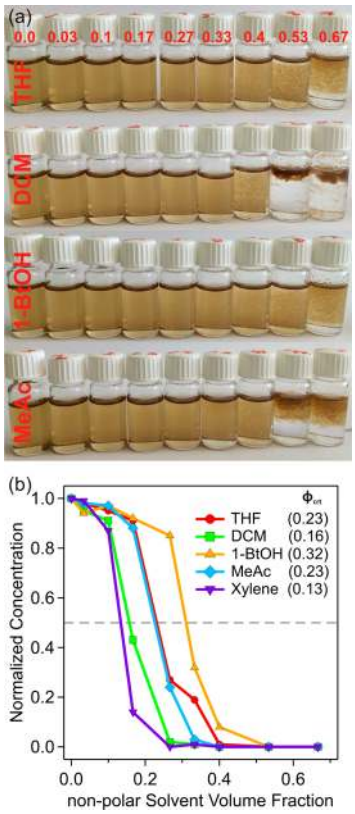

Figure 7. (a) Images of dispersions of GO (0.1 mg/mL) in a mixture of NMP and nonpolar solvents at different volume fractions of nonpolar solvents. Images are taken a day after preparation. (b) Normalized concentration of GO against the volume fraction of nonpolar solvents. The φ_{crt} is ascribed to the volume fraction at which the normalized concentration is half (dashed line). The values for φ_{crt} are given for each solvent in parentheses.

where φ is the volume fraction. By inserting φ_{crt} and relevant ε into the above equation, it is found that ε_{crt} = 24.3 ± 0.8. This value is close to experimental results, where it is found that acetone ($\varepsilon_{acetone}$ = 20.7) is at the border of good solvents for GO.[17] These findings imply for the solvents with ε much lower than ε_{crt}, there is no chance to have stable "bare GO" colloids and employing organic functionalization or polymeric dispersant is mandatory.[1,4]

For GO dispersions in polar solvents, however, aggregation is expected by adding salt or acid to media. However, unpredicted stabilization is observed in some organic solvents (e.g., NMP, DMSO) when ionic strength of media increased even up to 1M.[17] This is in clear contradiction to the DLVO theory. Therefore, there must be non-DLVO forces in action between the GO sheets which are probably solvation forces.[14,31] The magnitude of these forces is determined by interaction of surface-solvent (A_s) and the size of solvent (λ) (see Theoretical Basis). The total interactions between GO sheets are assumed to be the sum of the vdW and the solvation forces. Implementing the solvent properties (n, λ, and A_s) into the model, we found that the energy minimum for NMP, DMSO and DMF is around 20−40 times lower than the case for water (Figure 8). Therefore, in the case of water, the solvation forces are not strong enough to overcome the vdW forces, and aggregation is expected.[31] The success of the organic solvents originates from the larger molecular size (compared to water) and strong enough interaction with GO. In addition, due to the

DOI: 10.1021/acs.langmuir.6b01012
Langmuir 2016, 32, 5058−5068

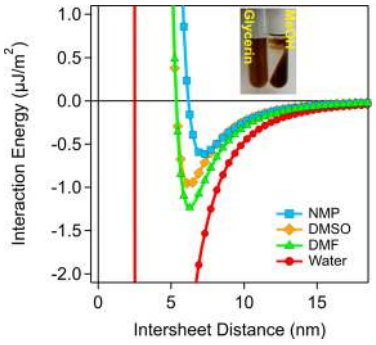

Figure 8. Interaction energy between two parallel GO sheets in different solvents in the absence of electrostatic forces but presence of solvation forces. Insets are images of GO dispersions in methanol and glycerin (1 mg/mL) containing 1 M of HCl.

higher refractive indices (n) of these solvents compared to water, the magnitude of the vdW interactions is around 2 times lower compared to aqueous system, which makes solvation stabilization even more feasible in the case of the organic solvents (Figure 8, Table 1).

The stability of GO in organic solvents, then, should be a function of the size of the solvents' molecules. Therefore, even polar protic solvents (e.g., alcohols) must be able to stabilize GO at high salt or acid concentration if the molecular size is large enough. To verify this, we prepared GO dispersions in methanol ($\lambda \sim 4$ Å) and glycerin ($\lambda \sim 5$ Å) through the "solvent exchange" method. GO sheets show high stability in glycerin at high acid concentration (1 M of HCl) (even after 1 h of centrifuging at 6000 rpm), whereas clear precipitation of GO is observed in the case of methanol (Figure 8). Despite the initial hypothesis in our previous work,[17] it is now concluded that solvent-stabilization of GO is dominated by the molecular size of solvents rather than their chemistry, unless high polarity is prerequisite. Although bulkier solvents are proposed to be more efficient for stabilization, the impact of the shape of the solvent molecules might be minor. From a practical point of view, this finding provides a basis for selecting suitable dispersing medium for GO, especially if the stability of single-layered GO matters. For instance, synthesis of metal(oxide)-GO hybrid usually involves using metal salts as precursors in solution.[65]

Other 2D Colloids. Extraordinary properties of the 2D materials provide a motive for material science communities to develop production methods in large scales.[11] Wet processing of the 2D materials in the form of the colloidal dispersions has attracted a great deal of attention.[1,10,11] Having stable dispersions of the 2D colloids is crucial for production, processing, and performance of final products. The accuracy of the DLVO theory, to predict colloidal properties of the 2D colloids, depends on employing proper force laws and physical constants for these novel materials. However, our findings may be relevant qualitatively. For instance, the analysis above tells us that thinner 2D colloids are less prone to aggregation due to the lower vdW interaction among them.[31,66] Another factor is the physical properties of the 2D colloids. The cases of GO and rGO showed that the vdW forces are sensitive to the intrinsic properties of the 2D colloids, especially the refractive index.[24] Another important parameter is the source of repulsive forces among the 2D colloids. In the case of aqueous dispersions, electrostatic forces are usually dominating, but the source of surface charge and the density of the charged species is system-dependent.[10,11] Besides the practical applications, study of the surface forces among atomically thin objects may raise some fundamental questions about intermolecular interactions at the 2D limit.

CONCLUSION

The dimensionality of the colloidal particles affects their colloidal properties and aggregation behavior. The case of GO and rGO showed that the DLVO theory can capture the interaction among them if proper force laws apply. More accurate Hamaker constants and vdW energy scaling laws were calculated, which makes quantitative prediction of the aggregation behavior of GO and rGO possible. Manner of aggregation of GO and rGO deviated from perfect 2D situation, which may originate from the finite thickness of them and/or probably breakdown of pairwise additive approximation at nanoscale.[52] Peculiar swelling and ordering of 2D colloids is predicted to arise from these nontrivial vdW interaction energy power laws. It is also found that the surface charge densities (σ) of GO and rGO are largely affected by pH. However, the changes in σ have less impact on the aggregation of GO (and in general 2D colloids) compared to spherical colloids. In addition, unlike spherical particles where size has negligible effect on the aggregation,[67] increasing the thickness of the 2D colloids is predicted to have profound effect on their stability.

Study of the aggregation of GO in organic solvents also revealed that there is a threshold for polarity of dispersing media to provide electrostatic stabilization for GO sheets. Therefore, there is no chance for the nonpolar solvents to accommodate stable monolayer GO sheets without adding stabilizer. On other hand, if the size of polar solvent molecules is big enough, solvation stabilization prevents the aggregation of the GO sheets even after adding huge amount of ions.

ASSOCIATED CONTENT

Supporting Information

The Supporting Information is available free of charge on the ACS Publications website at DOI: 10.1021/acs.langmuir.6b01012.

Calculation of 2D and 3D vdW interactions between graphene sheets, vdW power laws, estimation of GO and rGO thickness, and AFM images of GO sheets (PDF)

AUTHOR INFORMATION

Corresponding Author

*E-mail: mohsen.moazzami@unige.ch.

Present Address

†Department of Inorganic and Analytical Chemistry, University of Geneva, Science II, 30, Qui Ernest-Ansermet, Geneva 1211, Switzerland

Notes

The authors declare no competing financial interest.

ACKNOWLEDGMENTS

I would like to thanks Dr Seyed Hamed Aboutalebi and M M H Mohamadzadeh for helpful discussion and assistance in sample preparations.

REFERENCES

(1) Park, S.; Ruoff, R. S. Chemical methods for the production of graphenes. *Nat. Nanotechnol.* **2009**, *4*, 217−224.

DOI: 10.1021/acs.langmuir.6b01012
Langmuir 2016, 32, 5058−5068

(2) Eda, G.; Chhowalla, M. Chemically Derived Graphene Oxide: Towards Large-Area Thin-Film Electronics and Optoelectronics. *Adv. Mater.* **2010**, *22*, 2392−2415.
(3) Liu, Z.; Robinson, J. T.; Sun, X.; Dai, H. PEGylated Nanographene Oxide for Delivery of Water-Insoluble Cancer Drugs. *J. Am. Chem. Soc.* **2008**, *130*, 10876−10877.
(4) Stankovich, S.; Dikin, D. A.; Dommett, G. H. B.; Kohlhaas, K. M.; Zimney, E. J.; Stach, E. A.; Piner, R. D.; Nguyen, S. T.; Ruoff, R. S. Graphene-based composite materials. *Nature* **2006**, *442*, 282−286.
(5) Li, D.; Muller, M. B.; Gilje, S.; Kaner, R. B.; Wallace, G. G. Processable aqueous dispersions of graphene nanosheets. *Nat. Nanotechnol.* **2008**, *3*, 101−105.
(6) Shih, C.-J.; Lin, S.; Sharma, R.; Strano, M. S.; Blankschtein, D. Understanding the pH-Dependent Behavior of Graphene Oxide Aqueous Solutions: A Comparative Experimental and Molecular Dynamics Simulation Study. *Langmuir* **2012**, *28*, 235−241.
(7) Chowdhury, I.; Duch, M. C.; Mansukhani, N. D.; Hersam, M. C.; Bouchard, D. Colloidal Properties and Stability of Graphene Oxide Nanomaterials in the Aquatic Environment. *Environ. Sci. Technol.* **2013**, *47*, 6288−6296.
(8) Brodie, B. C. On the Atomic Weight of Graphite. *Philosophical Transactions of the Royal Society of London* **1859**, *149*, 249−259.
(9) Verwey, E. J. W.; Overbeek, J. T. G.; Overbeek, J. T. G. *Theory of the Stability of Lyophobic Colloids*; Courier Corporation: North Chelmsford, MA, 1999.
(10) Lotya, M.; Hernandez, Y.; King, P. J.; Smith, R. J.; Nicolosi, V.; Karlsson, L. S.; Blighe, F. M.; De, S.; Wang, Z.; McGovern, I. T.; Duesberg, G. S.; Coleman, J. N. Liquid Phase Production of Graphene by Exfoliation of Graphite in Surfactant/Water Solutions. *J. Am. Chem. Soc.* **2009**, *131*, 3611−3620.
(11) Nicolosi, V.; Chhowalla, M.; Kanatzidis, M. G.; Strano, M. S.; Coleman, J. N. Liquid Exfoliation of Layered Materials. *Science* **2013**, *340*, 1226419.
(12) Stankovich, S.; Dikin, D. A.; Piner, R. D.; Kohlhaas, K. A.; Kleinhammes, A.; Jia, Y.; Wu, Y.; Nguyen, S. T.; Ruoff, R. S. Synthesis of graphene-based nanosheets via chemical reduction of exfoliated graphite oxide. *Carbon* **2007**, *45*, 1558−1565.
(13) Chua, C. K.; Pumera, M. Chemical reduction of graphene oxide: a synthetic chemistry viewpoint. *Chem. Soc. Rev.* **2014**, *43*, 291−312.
(14) Israelachvili, J. N. *Intermolecular and Surface Forces: Revised Third Ed.*; Academic press: Waltham, MA, 2011.
(15) Derjaguin, B.; Landau, L. Theory of the stability of strongly charged lyophobic sols and of the adhesion of strongly charged particles in solutions of electrolytes. *Acta Physicochim. URSS* **1941**, *14*, 633−662.
(16) Li, Z.; Wang, Y.; Kozbial, A.; Shenoy, G.; Zhou, F.; McGinley, R.; Ireland, P.; Morganstein, B.; Kunkel, A.; Surwade, S. P.; Li, L.; Liu, H. Effect of airborne contaminants on the wettability of supported graphene and graphite. *Nat. Mater.* **2013**, *12*, 925−931.
(17) Gudarzi, M. M.; Moghadam, M. H. M.; Sharif, F. Spontaneous exfoliation of graphite oxide in polar aprotic solvents as the route to produce graphene oxide − organic solvents liquid crystals. *Carbon* **2013**, *64*, 403−415.
(18) Gobre, V. V.; Tkatchenko, A. Scaling laws for van der Waals interactions in nanostructured materials. *Nat. Commun.* **2013**, *4*, 2341.
(19) De Rocco, A. G.; Hoover, W. G. On the interaction of colloidal particles. *Proc. Natl. Acad. Sci. U. S. A.* **1960**, *46*, 1057−1065.
(20) Wang, S.; Zhang, Y.; Abidi, N.; Cabrales, L. Wettability and Surface Free Energy of Graphene Films. *Langmuir* **2009**, *25*, 11078−11081.
(21) Feriancikova, L.; Xu, S. Deposition and remobilization of graphene oxide within saturated sand packs. *J. Hazard. Mater.* **2012**, *235−236*, 194−200.
(22) Li, Y.; Wu, Y. Coassembly of Graphene Oxide and Nanowires for Large-Area Nanowire Alignment. *J. Am. Chem. Soc.* **2009**, *131*, 5851−5857.
(23) Parsegian, V. A. *Van der Waals Forces: A Handbook for Biologists, Chemists, Engineers, and Physicists*; Cambridge University Press: Cambridge, U.K., 2005.
(24) Jung, I.; Vaupel, M.; Pelton, M.; Piner, R.; Dikin, D. A.; Stankovich, S.; An, J.; Ruoff, R. S. Characterization of Thermally Reduced Graphene Oxide by Imaging Ellipsometry. *J. Phys. Chem. C* **2008**, *112*, 8499−8506.
(25) Rajter, R. F.; French, R. H.; Ching, W. Y.; Carter, W. C.; Chiang, Y. M. Calculating van der Waals-London dispersion spectra and Hamaker coefficients of carbon nanotubes in water from ab initio optical properties. *J. Appl. Phys.* **2007**, *101*, 054303.
(26) Girifalco, L. A.; Hodak, M.; Lee, R. S. Carbon nanotubes, buckyballs, ropes, and a universal graphitic potential. *Phys. Rev. B: Condens. Matter Mater. Phys.* **2000**, *62*, 13104−13110.
(27) Wu, L.; Liu, L.; Gao, B.; Muñoz-Carpena, R.; Zhang, M.; Chen, H.; Zhou, Z.; Wang, H. Aggregation Kinetics of Graphene Oxides in Aqueous Solutions: Experiments, Mechanisms, and Modeling. *Langmuir* **2013**, *29*, 15174−15181.
(28) Hua, Z.; Tang, Z.; Bai, X.; Zhang, J.; Yu, L.; Cheng, H. Aggregation and resuspension of graphene oxide in simulated natural surface aquatic environments. *Environ. Pollut.* **2015**, *205*, 161−169.
(29) Behrens, S. H.; Christl, D. I.; Emmerzael, R.; Schurtenberger, P.; Borkovec, M. Charging and Aggregation Properties of Carboxyl Latex Particles: Experiments versus DLVO Theory. *Langmuir* **2000**, *16*, 2566−2575.
(30) Konkena, B.; Vasudevan, S. Understanding Aqueous Dispersibility of Graphene Oxide and Reduced Graphene Oxide through pKa Measurements. *J. Phys. Chem. Lett.* **2012**, *3*, 867−872.
(31) Shih, C.-J.; Lin, S.; Strano, M. S.; Blankschtein, D. Understanding the Stabilization of Liquid-Phase-Exfoliated Graphene in Polar Solvents: Molecular Dynamics Simulations and Kinetic Theory of Colloid Aggregation. *J. Am. Chem. Soc.* **2010**, *132*, 14638−14648.
(32) Dubin, S.; Gilje, S.; Wang, K.; Tung, V. C.; Cha, K.; Hall, A. S.; Farrar, J.; Varshneya, R.; Yang, Y.; Kaner, R. B. A One-Step, Solvothermal Reduction Method for Producing Reduced Graphene Oxide Dispersions in Organic Solvents. *ACS Nano* **2010**, *4*, 3845−3852.
(33) Guo, Y.; Deng, L.; Li, J.; Guo, S.; Wang, E.; Dong, S. Hemin−Graphene Hybrid Nanosheets with Intrinsic Peroxidase-like Activity for Label-free Colorimetric Detection of Single-Nucleotide Polymorphism. *ACS Nano* **2011**, *5*, 1282−1290.
(34) Brown, M. A.; Abbas, Z.; Kleibert, A.; Green, R. G.; Goel, A.; May, S.; Squires, T. M. Determination of Surface Potential and Electrical Double-Layer Structure at the Aqueous Electrolyte-Nanoparticle Interface. *Phys. Rev. X* **2016**, *6*, 011007.
(35) Zhao, J.; Liu, F.; Wang, Z.; Cao, X.; Xing, B. Heteroaggregation of Graphene Oxide with Minerals in Aqueous Phase. *Environ. Sci. Technol.* **2015**, *49*, 2849−2857.
(36) Eigler, S.; Dotzer, C.; Hof, F.; Bauer, W.; Hirsch, A. Sulfur Species in Graphene Oxide. *Chem. - Eur. J.* **2013**, *19*, 9490−9496.
(37) Martinez, C. R.; Iverson, B. L. Rethinking the term ″pi-stacking″. *Chemical Science* **2012**, *3*, 2191−2201.
(38) Yang, L.; Brazier, J. B.; Hubbard, T. A.; Rogers, D. M.; Cockroft, S. L. Can Dispersion Forces Govern Aromatic Stacking in an Organic Solvent? *Angew. Chem., Int. Ed.* **2016**, *55*, 912−916.
(39) Park, S.; Hu, Y.; Hwang, J. O.; Lee, E.-S.; Casabianca, L. B.; Cai, W.; Potts, J. R.; Ha, H.-W.; Chen, S.; Oh, J.; Kim, S. O.; Kim, Y.-H.; Ishii, Y.; Ruoff, R. S. Chemical structures of hydrazine-treated graphene oxide and generation of aromatic nitrogen doping. *Nat. Commun.* **2012**, *3*, 638.
(40) Zhang, J.; Yang, H.; Shen, G.; Cheng, P.; Zhang, J.; Guo, S. Reduction of graphene oxide vial-ascorbic acid. *Chem. Commun.* **2010**, *46*, 1112−1114.
(41) Wang, Y.; Shi, Z.; Yin, J. Facile Synthesis of Soluble Graphene via a Green Reduction of Graphene Oxide in Tea Solution and Its Biocomposites. *ACS Appl. Mater. Interfaces* **2011**, *3*, 1127−1133.
(42) Ma, Q.; Song, J.; Jin, C.; Li, Z.; Liu, J.; Meng, S.; Zhao, J.; Guo, Y. A rapid and easy approach for the reduction of graphene oxide by formamidinesulfinic acid. *Carbon* **2013**, *54*, 36−41.
(43) Bose, S.; Kuila, T.; Mishra, A. K.; Kim, N. H.; Lee, J. H. Dual role of glycine as a chemical functionalizer and a reducing agent in the

DOI: 10.1021/acs.langmuir.6b01012
Langmuir 2016, 32, 5058−5068

preparation of graphene: an environmentally friendly method. *J. Mater. Chem.* **2012**, *22*, 9696−9703.
(44) Zhu, C.; Guo, S.; Fang, Y.; Dong, S. Reducing Sugar: New Functional Molecules for the Green Synthesis of Graphene Nanosheets. *ACS Nano* **2010**, *4*, 2429−2437.
(45) You, S.; Luzan, S. M.; Szabó, T.; Talyzin, A. V. Effect of synthesis method on solvation and exfoliation of graphite oxide. *Carbon* **2013**, *52*, 171−180.
(46) Chowdhury, I.; Mansukhani, N. D.; Guiney, L. M.; Hersam, M. C.; Bouchard, D. Aggregation and Stability of Reduced Graphene Oxide: Complex Roles of Divalent Cations, pH, and Natural Organic Matter. *Environ. Sci. Technol.* **2015**, *49*, 10886−10893.
(47) Chowdhury, I.; Duch, M. C.; Mansukhani, N. D.; Hersam, M. C.; Bouchard, D. Deposition and Release of Graphene Oxide Nanomaterials Using a Quartz Crystal Microbalance. *Environ. Sci. Technol.* **2014**, *48*, 961−969.
(48) Dimiev, A. M.; Alemany, L. B.; Tour, J. M. Graphene Oxide. Origin of Acidity, Its Instability in Water, and a New Dynamic Structural Model. *ACS Nano* **2013**, *7*, 576−588.
(49) Shih, C.-J.; Lin, S.; Strano, M. S.; Blankschtein, D. Understanding the Stabilization of Single-Walled Carbon Nanotubes and Graphene in Ionic Surfactant Aqueous Solutions: Large-Scale Coarse-Grained Molecular Dynamics Simulation-Assisted DLVO Theory. *J. Phys. Chem. C* **2015**, *119*, 1047−1060.
(50) Aich, N.; Boateng, L. K.; Sabaraya, I. V.; Das, D.; Flora, J. R. V.; Saleh, N. B. Aggregation Kinetics of Higher-Order Fullerene Clusters in Aquatic Systems. *Environ. Sci. Technol.* **2016**, *50*, 3562−3571.
(51) Trefalt, G.; Szilagyi, I.; Borkovec, M. Poisson−Boltzmann description of interaction forces and aggregation rates involving charged colloidal particles in asymmetric electrolytes. *J. Colloid Interface Sci.* **2013**, *406*, 111−120.
(52) Ambrosetti, A.; Ferri, N.; DiStasio, R. A.; Tkatchenko, A. Wavelike charge density fluctuations and van der Waals interactions at the nanoscale. *Science* **2016**, *351*, 1171−1176.
(53) Spector, M. S.; Naranjo, E.; Chiruvolu, S.; Zasadzinski, J. A. Conformations of a Tethered Membrane: Crumpling in Graphitic Oxide? *Phys. Rev. Lett.* **1994**, *73*, 2867−2870.
(54) Wen, X.; Garland, C. W.; Hwa, T.; Kardar, M.; Kokufuta, E.; Li, Y.; Orkisz, M.; Tanaka, T. Crumpled and collapsed conformation in graphite oxide membranes. *Nature* **1992**, *355*, 426−428.
(55) Meyer, J. C.; Geim, A. K.; Katsnelson, M. I.; Novoselov, K. S.; Booth, T. J.; Roth, S. The structure of suspended graphene sheets. *Nature* **2007**, *446*, 60−63.
(56) Norrish, K. Crystalline Swelling of Montmorillonite: Manner of Swelling of Montmorillonite. *Nature* **1954**, *173*, 256−257.
(57) Walker, G. F. Macroscopic Swelling of Vermiculite Crystals in Water. *Nature* **1960**, *187*, 312−313.
(58) Norrish, K. The swelling of montmorillonite. *Discuss. Faraday Soc.* **1954**, *18*, 120−134.
(59) Geng, F.; Ma, R.; Nakamura, A.; Akatsuka, K.; Ebina, Y.; Yamauchi, Y.; Miyamoto, N.; Tateyama, Y.; Sasaki, T. Unusually stable ∼ 100-fold reversible and instantaneous swelling of inorganic layered materials. *Nat. Commun.* **2013**, *4*, 1632.
(60) Yang, X.; Qiu, L.; Cheng, C.; Wu, Y.; Ma, Z.-F.; Li, D. Ordered Gelation of Chemically Converted Graphene for Next-Generation Electroconductive Hydrogel Films. *Angew. Chem., Int. Ed.* **2011**, *50*, 7325−7328.
(61) Van Der Hoeven, P. C.; Lyklema, J. Electrostatic stabilization in non-aqueous media. *Adv. Colloid Interface Sci.* **1992**, *42*, 205−277.
(62) Jalili, R.; Aboutalebi, S. H.; Esrafilzadeh, D.; Konstantinov, K.; Moulton, S. E.; Razal, J. M.; Wallace, G. G. Organic Solvent-Based Graphene Oxide Liquid Crystals: A Facile Route toward the Next Generation of Self-Assembled Layer-by-Layer Multifunctional 3D Architectures. *ACS Nano* **2013**, *7*, 3981−3990.
(63) Briscoe, W. H.; Horn, R. G. Direct Measurement of Surface Forces Due to Charging of Solids Immersed in a Nonpolar Liquid. *Langmuir* **2002**, *18*, 3945−3956.
(64) Jouyban, A.; Soltanpour, S.; Chan, H.-K. A simple relationship between dielectric constant of mixed solvents with solvent composition and temperature. *Int. J. Pharm.* **2004**, *269*, 353−360.
(65) Wang, D.; Kou, R.; Choi, D.; Yang, Z.; Nie, Z.; Li, J.; Saraf, L. V.; Hu, D.; Zhang, J.; Graff, G. L.; Liu, J.; Pope, M. A.; Aksay, I. A. Ternary Self-Assembly of Ordered Metal Oxide−Graphene Nanocomposites for Electrochemical Energy Storage. *ACS Nano* **2010**, *4*, 1587−1595.
(66) Kang, J.; Seo, J.-W. T.; Alducin, D.; Ponce, A.; Yacaman, M. J.; Hersam, M. C. Thickness sorting of two-dimensional transition metal dichalcogenides via copolymer-assisted density gradient ultracentrifugation. *Nat. Commun.* **2014**, *5*, 5478.
(67) Elimelech, M.; O'Melia, C. R. Effect of particle size on collision efficiency in the deposition of Brownian particles with electrostatic energy barriers. *Langmuir* **1990**, *6*, 1153−1163.

DOI: 10.1021/acs.langmuir.6b01012
Langmuir 2016, 32, 5058−5068